

## Original Article

# Development of a clinically feasible [<sup>11</sup>C]PE2I PET method for differential diagnosis of parkinsonism using reduced scan duration and automated reference region extraction

My Jonasson<sup>1,2</sup>, Lieuwe Appel<sup>1,3</sup>, Torsten Danfors<sup>1,3</sup>, Dag Nyholm<sup>4</sup>, Håkan Askmark<sup>4</sup>, Andreas Frick<sup>5</sup>, Jonas Engman<sup>5</sup>, Tomas Furmark<sup>5</sup>, Jens Sörensen<sup>1,3</sup>, Mark Lubberink<sup>1,2</sup>

<sup>1</sup>Nuclear Medicine and PET, Department of Surgical Sciences, Uppsala University, Uppsala, Sweden; <sup>2</sup>Medical Physics, Uppsala University Hospital, Uppsala, Sweden; <sup>3</sup>PET Centre, Uppsala University Hospital, Uppsala, Sweden; <sup>4</sup>Neurology, Department of Neuroscience, Uppsala University, Uppsala, Sweden; <sup>5</sup>Department of Psychology, Uppsala University, Uppsala, Sweden

Received November 3, 2017; Accepted November 21, 2017; Epub December 20, 2017; Published December 30, 2017

**Abstract:** [<sup>11</sup>C]PE2I is a highly selective dopamine transporter PET ligand. Parametric images based on dynamic [<sup>11</sup>C]PE2I scans, showing dopamine transporter availability ( $BP_{ND}$ ) and relative cerebral blood flow ( $R_1$ ), can be used in differential diagnosis of parkinsonism. This work aimed to investigate a shortened scan duration and automated generation of parametric images which are two prerequisites for routine clinical application. Twelve subjects with parkinsonism and seventeen healthy controls underwent 80 min dynamic [<sup>11</sup>C]PE2I PET scans.  $BP_{ND}$  and  $R_1$  images were generated using cerebellum reference region defined on a co-registered MRI, as well as a supervised cluster analysis (SVCA)-based reference. Initial 20, 30 and 40 min of the scans were extracted and images of standardized uptake value ratio (SUVR) and  $R_1$  were computed using MRI- and SVCA-based reference. Correlation was high between striatal 80 min MRI-based  $BP_{ND}$  and 40 min SVCA-based SUVR-1 ( $R^2=0.95$ ). High correlation was also found between  $R_1$  values in striatal and limbic regions ( $R^2\geq 0.91$ ) whereas correlation was moderate for cortical regions ( $R^2=0.71$ ). The results indicate that dynamic [<sup>11</sup>C]PE2I scans can be restricted to 40 min and that SVCA can be used for automatic extraction of a reference region. These outcomes will support routine applications of [<sup>11</sup>C]PE2I PET in clinical settings.

**Keywords:** PET, [<sup>11</sup>C]PE2I, parkinsonism, parametric images, supervised clustering

## Introduction

Parkinsonism is a clinical syndrome characterized by bradykinesia, rigidity, tremor and postural instability. It is most commonly caused by Parkinson's disease (PD) but there are other neurological conditions such as multiple system atrophy (MSA), progressive supranuclear palsy, corticobasal degeneration and dementia with Lewy bodies, with overlapping clinical symptoms. In addition, there are some non-neurodegenerative disorders such as vascular parkinsonism and drug-induced parkinsonism with symptoms resembling PD. Differential diagnosis can be difficult to obtain based on clinical symptoms, but is of great importance to

be able to provide patients with correct prognosis and choice of treatment.

The dopamine transporter (DAT) is a transmembrane protein responsible for the reuptake of dopamine in the synaptic cleft. Decreased DAT availability is associated with various neurological disorders such as Parkinson's disease [1, 2]. The carbon-11 labelled cocaine analog N-(3-iodoprop-2E-enyl)-2 $\beta$ -carbomethoxy-3 $\beta$ -(4-methyl-phenyl)nortropane ([<sup>11</sup>C]PE2I) is an established positron emission tomography (PET) ligand for imaging of DAT and has shown a marked accumulation in the striatum where the concentration of DAT is high [3-7]. A straightforward visual assessment of DAT availability can

be provided by parametric images where the binding potential ( $\text{BP}_{\text{ND}}$ ) is estimated for each voxel. Recently, we demonstrated that a basis function approach of the simplified reference tissue method (SRTM) [8], receptor parametric mapping (RPM) [9], using cerebellum as reference region, is the preferred method for producing  $\text{BP}_{\text{ND}}$  and relative delivery ( $R_1$ ) images of [ $^{14}\text{C}$ ]PE2I [10]. The  $R_1$  images reflect regional cerebral blood flow which is a measure of overall brain functional activity. A combination of [ $^{14}\text{C}$ ]PE2I  $\text{BP}_{\text{ND}}$  and  $R_1$  has been proposed to replace the current dual scan approach with [ $^{123}\text{I}$ ]FP-CIT SPECT, showing DAT availability, and [ $^{18}\text{F}$ ]FDG PET or [ $^{99\text{m}}\text{Tc}$ ]HMPAO SPECT, expressing overall brain functional activity or blood flow, respectively, for accurate differential diagnosis of patients with parkinsonism [11]. Benefits of the use of [ $^{14}\text{C}$ ]PE2I are improved patient logistics, a lower radiation dose and possibly decreased costs, as well as quantitative measures of DAT availability and overall brain functional activity.

For clinical application of [ $^{14}\text{C}$ ]PE2I PET as a routine method for differential diagnosis of parkinsonian disorders, there is need for further development of the scanning protocol and data evaluation methods. Previous validation studies [10, 11] have been based on an acquisition of an 80 min [ $^{14}\text{C}$ ]PE2I PET scan since it has been demonstrated that such a scan duration is necessary for robust determination of  $\text{BP}_{\text{ND}}$  [3-5]. However, an 80 min scan duration is not suitable for routine clinical use in a patient group suffering from movement disorders and it would be of great clinical relevance to be able to shorten the scan protocol. It has previously been shown that  $\text{BP}_{\text{ND}}$  can be estimated as the ratio of the activity concentrations in target and reference regions at transient equilibrium which is the time at which the specific binding, calculated as the difference between target and reference region curves, peaks [12]. This occurs probably much earlier than after 80 min and would therefore offer an opportunity for reduced scan duration whilst still resulting in quantitative measures of DAT availability. It should also be validated whether accurate estimation of  $R_1$  is still possible at these shorter scan durations.

Another challenge associated with clinical use of dynamic [ $^{14}\text{C}$ ]PE2I is the need to define a reference region volume of interest (VOI) for gen-

eration of parametric images. In previous work this was done using a co-registered structural MRI scan which meant an additional scan for the patient [11], or by manually drawing the region, which is time consuming. Both would limit the clinical feasibility of using [ $^{14}\text{C}$ ]PE2I. An automatic approach to extract a reference time activity curve (TAC) directly from the dynamic PET data is the supervised cluster analysis (SVCA) method [13] which has previously been suggested for (R)-[ $^{14}\text{C}$ ]PK11195 [13, 14], [ $^{14}\text{C}$ ]PIB [15], [ $^{14}\text{C}$ ](R)-rolipram [16] and [ $^{14}\text{C}$ ]TMSX [17] and has demonstrated a robust and reliable alternative to traditional template-based or manual definition of reference regions. The SVCA algorithm segments voxels in the dynamic PET volume based on their time activity curves with no spatial constraint, i.e. the whole brain. Voxels with TACs most resembling the kinetic behaviour of the proposed reference region are selected and a reference TAC can be obtained. Although the principles of an implementation of the SVCA algorithm are similar for each tracer, this method needs to be validated for [ $^{14}\text{C}$ ]PE2I.

The aims of the present study were therefore: (1) to investigate a shortened acquisition time for determination of both DAT availability and overall brain functional activity, and (2) to validate a supervised cluster analysis method for automatic extraction of a reference time activity curve directly from the dynamic [ $^{14}\text{C}$ ]PE2I data in order to enable automated generation of DAT availability and overall brain functional activity images.

## Materials and methods

### Subjects

Data from 29 subjects were included in this study: 12 subjects clinically diagnosed with parkinsonism (7 women and 5 men, mean age  $70 \pm 6$  years), 12 healthy controls (HC; 4 women and 8 men, mean age  $47 \pm 8$  years) and 5 additional healthy subjects (men, mean age  $25 \pm 4$  years) included as a separate set of data for definition of kinetic classes in the SVCA algorithm. The 12 subjects with parkinsonism all had notable reduction in striatal DAT availability based on [ $^{14}\text{C}$ ]PE2I  $\text{BP}_{\text{ND}}$  images and their characteristics have been described previously by Appel et al. [11]. Written informed consent was obtained from each subject and the study was

approved by the regional board of medical ethics in Uppsala.

#### *Data acquisition*

[<sup>11</sup>C]PE2I was synthesized using previously described methods [4, 18]. Each subject underwent a dynamic [<sup>11</sup>C]PE2I PET scan on an ECAT Exact HR+ scanner (Siemens/CTI, Knoxville). A 10 min transmission scan with rotating <sup>68</sup>Ge rod sources was performed for attenuation correction. Then, an 80 min emission scan in 3-dimensional acquisition mode was started simultaneously with the injection of about 350 MBq [<sup>11</sup>C]PE2I. Twenty-two frames of increasing durations (4×1, 2×2, 4×3, 12×5 min) were acquired and dynamic images were reconstructed using ordered subset expectation maximization (OSEM) using 6 iterations and 8 subsets and a 4 mm Hanning post-filter, applying all appropriate corrections. In addition, each subject underwent a T1-weighted MRI scan (3D-SENSE) for anatomical information on either a 1.5 Tesla or a 3 Tesla Achieva scanner (Philips Healthcare, Best, The Netherlands).

#### *Image analysis*

Dynamic [<sup>11</sup>C]PE2I PET images were realigned to correct for inter-frame patient motion using VOIager (GE Healthcare, Uppsala, Sweden). The sum of the first three frames of the [<sup>11</sup>C]PE2I PET scan was used for co-registration of the MRI scan based on a 6-parameter rigid transformation and MR images were segmented into grey matter, white matter and CSF using statistical parametric mapping (SPM8; Wellcome Trust Center for Neuroimaging, University College London, UK). Grey matter VOIs were defined on the co-registered MR images applying an automated probabilistic VOI template as implemented in the PVElab software [19].

Parametric BP<sub>ND</sub> and R<sub>1</sub> images were generated using receptor parametric mapping (RPM) [9] with cerebellar grey matter as reference region. RPM is an implementation of SRTM [8] using a set of predefined basis functions to linearize the model and estimating BP<sub>ND</sub> and R<sub>1</sub> for each voxel. One hundred basis functions were predefined for each scan with a discrete set of values for the exponential variable ranging from 0.01 to 0.5 min<sup>-1</sup>. Weights were included in the data analysis to take into account the different counts in each frame.

#### *Acquisition time*

To evaluate the possibility of a shortened scan protocol, different durations of the acquired data were considered: the first 20 min (10 frames), 30 min (12 frames) and 40 min (14 frames) of the original 80 min [<sup>11</sup>C]PE2I data. Since scan durations as short as 40 min are not sufficient for BP<sub>ND</sub> calculations of [<sup>11</sup>C]PE2I [3, 4], DAT availability was approximated using standardized uptake value ratio (SUVr) images for the last two frames of each data set (14-20 min, 20-30 min and 30-40 min) and BP<sub>ND</sub> was estimated as SUVr-1. In addition, parametric R<sub>1</sub> images were generated for each shortened data set using RPM [10].

#### *Supervised cluster analysis*

A SVCA algorithm specific for [<sup>11</sup>C]PE2I was developed in Matlab (Mathworks, Natick MA). For this purpose, a set of five kinetic classes was predefined on dynamic [<sup>11</sup>C]PE2I data from the five healthy subjects, that were specifically included for this purpose only in order to have an unbiased evaluation of the subjects included in the analysis: grey matter cerebellum (corresponding to non-specific binding), striatum (corresponding to high specific binding), white matter, blood and a class to collect remaining voxels. The definition of the classes other than grey matter cerebellum was aimed at avoiding inclusion of their associated voxels in the cerebellum class. Cerebellum, striatum and white matter classes were defined using the MRI-based VOIs generated with PVElab. The blood class was defined as voxels with a value higher than 30% of the maximum voxel value during the initial 60 seconds (first frame) on the ten most caudal slices, and the class for the remaining voxels was defined as voxels with a value between 2% and 20% of the maximum value on a sum of the first six minutes (frames 1-5). The TACs from each class were normalized to their respective area under the curve.

In order to generate reference time-activity curves for each of the 12 patients with parkinsonism and 12 healthy controls, the TACs of each voxel in the dynamic data sets were normalized to their area under the curve. A non-negative least-squares algorithm was used to find a linear combination of the probability for each voxel to correspond to each kinetic class. Different limits of the probability of the voxels to belong to a class were investigated using five different thresholds; 0.7, 0.8, 0.9, 0.95 and 1.

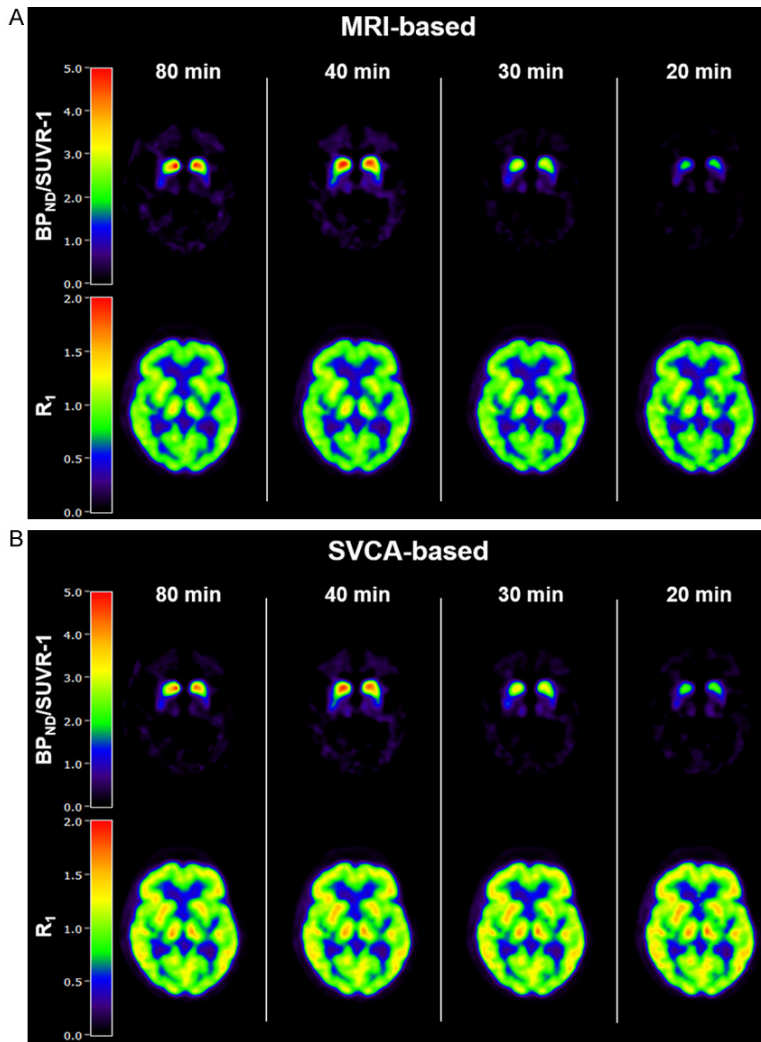


**Figure 1.** Parametric [<sup>11</sup>C]PE2I images of a patient with probable PD. A. Comparison of BP<sub>ND</sub> and SUVR-1 images (top row) and R<sub>1</sub> images (bottom row) of different scan durations with an MRI-based reference region. B. BP<sub>ND</sub> and SUVR-1 images (top row) and R<sub>1</sub> images (bottom row) of different scan duration with an SVCA-based reference region.

Voxels with a probability higher than, or equal to (in the case for 1), the threshold, were assigned to that specific class. The voxels selected for the cerebellum class were regarded as reference region and a mean of the TACs of the selected voxels was calculated. The SVCA-extracted reference TAC was then used as input function to generate new parametric BP<sub>ND</sub> and R<sub>1</sub> images for the full 80 min [<sup>11</sup>C]PE2I data and SUVR-1 and R<sub>1</sub> images for the shortened data sets.

#### Data evaluation

Quantitative evaluation was performed by retrieving regionally average voxel values by pro-

jecting the MRI-based VOIs, originating from PVELab, on the BP<sub>ND</sub>, SUVR-1 and R<sub>1</sub> images. For BP<sub>ND</sub> and SUVR-1, the evaluation was restricted to a striatal region (putamen and caudate nucleus). For R<sub>1</sub>, three sets of VOIs were analysed separately; striatum (putamen and caudate nucleus), a cortical group (frontal-, parietal-, occipital, somatosensory and motor cortex) and a limbic group (thalamus, hypothalamus, hippocampus and amygdala). Left and right sides of each VOI were used separately. BP<sub>ND</sub> and R<sub>1</sub> values based on 80 min [<sup>11</sup>C]PE2I data were considered as the established standard in the following comparisons related to reduced scan durations and use of SVCA. All statistical evaluations were performed using GraphPad Prism (GraphPad Software, La Jolla, Ca, USA).

#### Acquisition time

In the first step, BP<sub>ND</sub> and R<sub>1</sub> values of the complete 80 min data set with MRI-based reference (BP<sub>ND-MRI-80</sub>, R<sub>1-MRI-80</sub>) and SUVR-1 and R<sub>1</sub> values of the shortened data sets with MRI-based reference (SUVR-1<sub>MRI-20</sub>, SUVR-1<sub>MRI-30</sub>, SUVR-1<sub>MRI-40</sub> and R<sub>1-MRI-20</sub>, R<sub>1-MRI-30</sub> and R<sub>1-MRI-40</sub>) were compared. Correlation and agreement were assessed using the square of the correlation coefficient (R<sup>2</sup>) and slope of orthogonal regression.

#### Supervised cluster analysis

In the second step, relationships between the estimates of BP<sub>ND</sub> and R<sub>1</sub> with MRI- and SVCA-based reference, for the complete 80 min data set, were investigated, i.e. BP<sub>ND-MRI-80</sub> vs BP<sub>ND-SVCA-80</sub> and R<sub>1-MRI-80</sub> vs R<sub>1-SVCA-80</sub>. R<sup>2</sup> and slope of orthogonal regression analysis were used to compare the two reference methods. The different thresholds used for SVCA were evaluated in



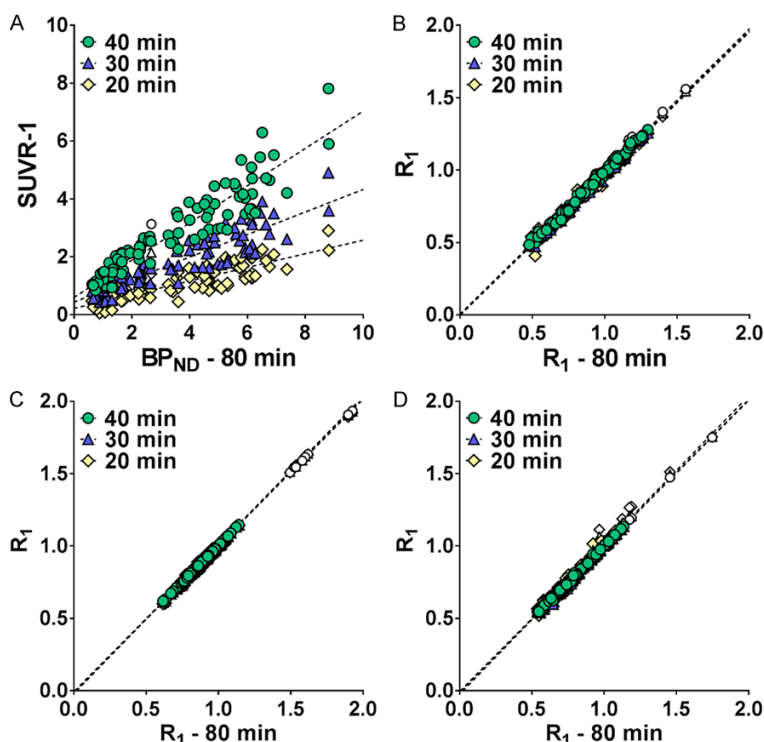


**Figure 2.** Relationship between 80 min acquisition time and extracted data limited to the first 20-40 min of (A) striatal  $BP_{ND}$  and SUVR-1 values, (B) striatal  $R_1$  values, (C) cortical  $R_1$  values and (D) limbic  $R_1$  values all based on an MRI-defined cerebellum reference region. Open symbols correspond to a parkinsonian subject with a probable diagnosis of MSA with atrophy in cerebellum and this subject is not included in the statistical analysis. For (B-D) the values of different scan durations are overlapping.

**Table 1.** Square of Pearson’s correlation coefficient ( $R^2$ ) and slope of orthogonal regression relative to 80 min  $BP_{ND}$  and  $R_1$

Acquisition time	Striatal SUVR-1		Striatal $R_1$		Cortical $R_1$		Limbic $R_1$	
	$R^2$	Slope	$R^2$	Slope	$R^2$	Slope	$R^2$	Slope
40 min	0.87	0.64*	0.99	0.98	1.00	1.01*	1.00	1.01
30 min	0.82	0.39*	0.99	0.98*	1.00	1.02*	0.99	1.01
20 min	0.78	0.24*	0.98	0.98	0.99	1.03*	0.98	1.03*

All values are based on an MRI-defined cerebellum reference region. \*: slope significantly different from 1.

terms of their accuracy in describing the MRI-based cerebellum TAC, calculated as the residual sum of squares (RSS). In addition,  $R^2$ , slope and bias were calculated between  $BP_{ND}$  and  $R_1$  values with MRI-based reference region and SVCA-based reference with different thresholds.

*Combination of shortened acquisition time and supervised cluster analysis*

To evaluate the combination of a shorter acquisition time and SVCA, values retrieved from

SUVR-1 and  $R_1$  images generated from the shortened data sets using SVCA-based reference ( $SUVR-1_{SVCA-20}$ ,  $SUVR-1_{SVCA-30}$ ,  $SUVR-1_{SVCA-40}$  and  $R_{1-SVCA-20}$ ,  $R_{1-SVCA-30}$ ,  $R_{1-SVCA-40}$ ) were compared to  $BP_{ND-MRI-80}$  and  $R_{1-MRI-80}$  respectively, calculating  $R^2$  and slope of orthogonal regression.

To evaluate the ability of each method to discriminate between groups, the standardized difference of the mean  $BP_{ND}$  and SUVR-1 values (Cohen’s d) between HC and subjects with parkinsonism was calculated for each scan duration with both MRI- and SVCA-based reference. Cohen’s d is calculated as the difference between the means of both groups divided by the pooled standard deviation. This gives the effect size expressed in number of pooled standard deviations and was used as a further indication of an acquisition time sufficient for determination of DAT availability.

**Results**

*Acquisition time*

Parametric images of SUVR-1 and  $R_1$  of the shortened data sets compared to 80 min  $BP_{ND}$  and  $R_1$  images from one parkinsonian subject are given in **Figure 1A** and from one HC in **Supplemental Figure 1A**. RPM

produced visually similar  $R_1$  images for the different scan durations while SUVR-1 values decreased with shorter scan duration but demonstrated the same pattern of DAT availability for all data sets.

Relationships between  $BP_{ND-MRI-80}$  values and  $SUVR-1_{MRI-20}$ ,  $SUVR-1_{MRI-30}$  and  $SUVR-1_{MRI-40}$  values in striatal regions, and between  $R_{1-MRI-80}$  values and  $R_{1-MRI-20}$ ,  $R_{1-MRI-30}$  and  $R_{1-MRI-40}$  values in striatal, cortical and limbic regions are shown in **Figure 2**, with the corresponding  $R^2$  and

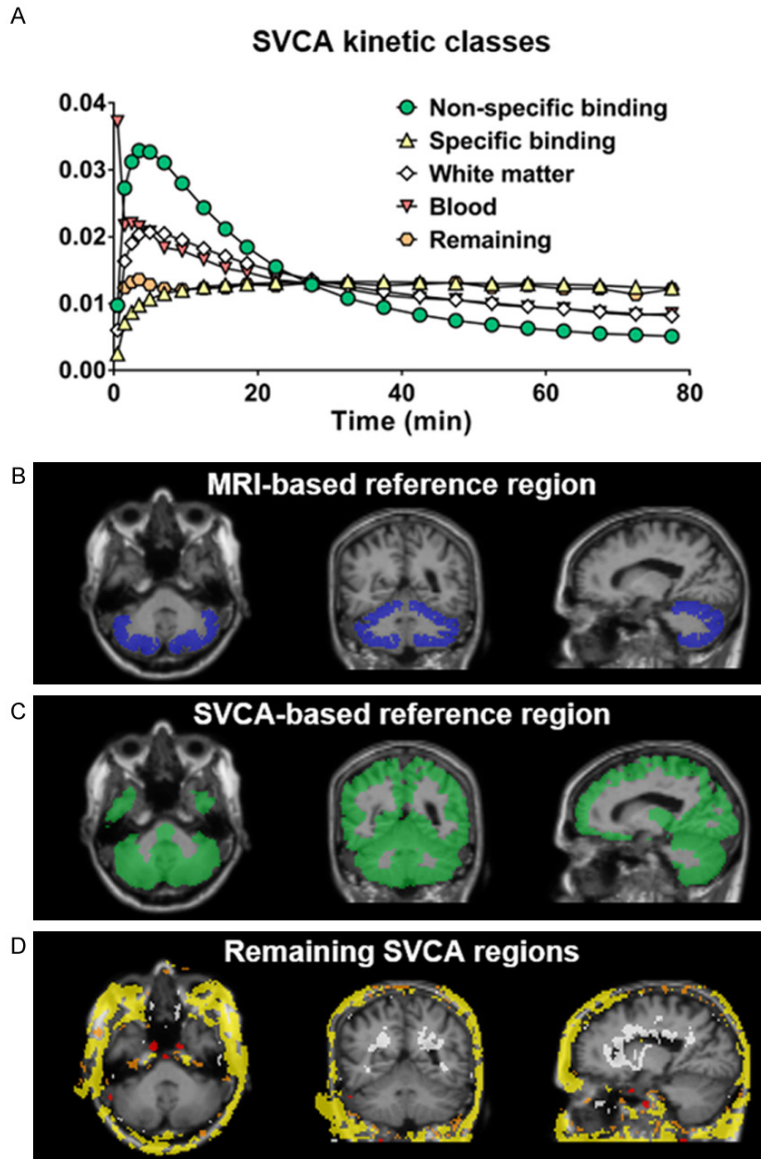


**Figure 3.** (A) Normalized time activity curves of the predefined kinetic classes used for SVCA, (B) MRI-based cerebellum reference region from PVElab, (C) SVCA extracted reference region, (D) the four remaining SVCA-regions.

slope values given in **Table 1**. Correlations between striatal  $BP_{ND-MRI-80}$  and  $SUVR-1_{MRI-30}$  and  $SUVR-1_{MRI-40}$  were high ( $R^2=0.82$  and  $0.87$  respectively), and slightly lower for  $SUVR-1_{MRI-20}$ . The slope values showed an underestimation of  $SUVR-1$  relative to  $BP_{ND-MRI-80}$  which increased with shorter scan duration. For  $R_1$  of the shortened data sets, the correlations and slope values were equal or close to one for all regions and scan durations compared to  $R_{1-MRI-80}$ . All correlations were significant ( $p<0.0001$ ).

In the regression plots of  $R_1$  (**Figure 2B-D**) a small number of values exceeding 1.5 are

clearly visible. These outliers correspond to a parkinsonian subject with a probable diagnosis of MSA with cerebellar atrophy. The lower uptake of tracer in cerebellum in this patient induces overall higher  $R_1$  values, but it does not affect the  $BP_{ND}$  values. However, data from this subject were excluded in all statistical analysis because it resulted in artificially high correlations when  $R_1$  values for different scan times were compared.

#### Supervised cluster analysis

The results of the evaluation of the different thresholds for SVCA are given in **Supplemental Table 1**. Mean RSS of all subjects was lowest for a threshold of 1 and gradually increased with decreasing threshold. For some individuals, a threshold equal to 1 only allowed very few voxels to be included in the reference region, and was thus discarded. High correlations were found between  $BP_{ND-MRI-80}$  and  $BP_{ND-SVCA-80}$  with different thresholds ( $R^2 \geq 0.98$ ) and slopes close to one, but large negative biases for thresholds of 0.9 and higher. Comparisons between  $R_{1-MRI-80}$  and  $R_{1-SVCA-80}$  with different thresholds gave a lower correlation ( $R^2$  between 0.85 and 0.89), with the largest bias for

a threshold of 0.7. As a compromise a threshold of 0.8 was chosen.

TACs of the five predefined kinetic classes are shown in **Figure 3A**. Reference regions obtained from the MRI-based template and from the SVCA-based method, with voxels corresponding to the non-specific binding class, are shown in **Figure 3B** and **3C** respectively and VOIs of remaining four SVCA classes are given in **Figure 3D**, for one subject. While the MRI-based reference VOI is limited to the cerebellum, the SVCA-based reference VOI also includes a substantial number of voxels in cortical regions, due to

Clinically feasible [<sup>11</sup>C]PE2I PET

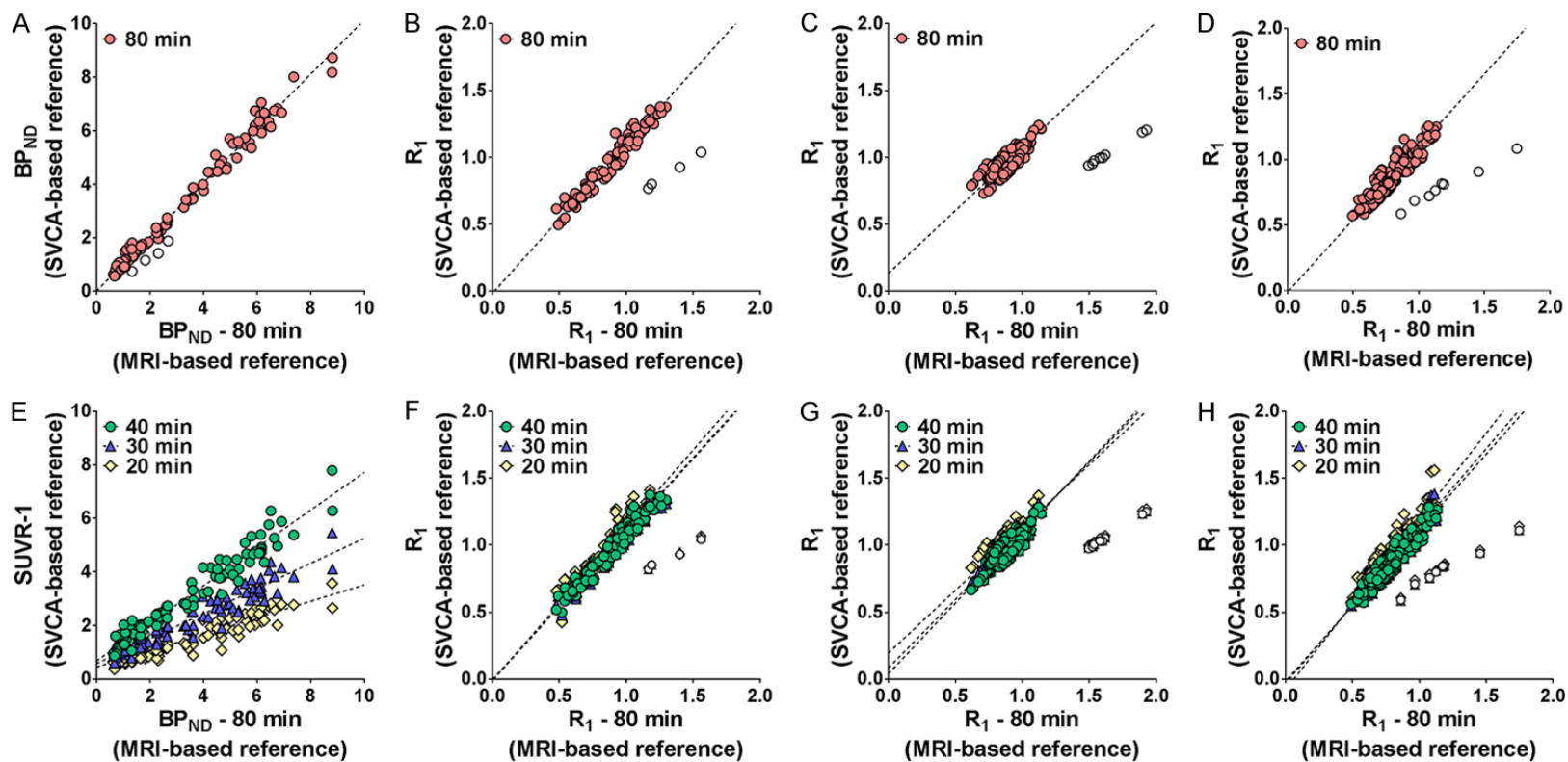


**Figure 4.** (A-D) Relationship between the full 80 min acquisition time with MRI- and SVCA-based reference for (A) striatal  $BP_{ND}$  values, (B) striatal  $R_1$  values, (C) cortical  $R_1$  values and (D) limbic  $R_1$  values. (E-H) Relationship between 80 min scan duration with MRI-based reference and extracted data limited to the first 20-40 min with SVCA-based reference of (E) striatal SUVR-1 values, (F) striatal  $R_1$  values, (G) cortical  $R_1$  values and (H)  $R_1$  values in limbic regions. Open symbols correspond to a parkinsonian subject with a probable diagnosis of MSA with atrophy in cerebellum and this subject is not included in the statistical analysis.

## Clinically feasible [<sup>11</sup>C]PE2I PET

**Table 2.** Square of Pearson's correlation coefficient ( $R^2$ ) and slope of orthogonal regression of  $BP_{ND}$ , SUVR-1 and  $R_1$  with SVCA-based reference region relative to 80 min  $BP_{ND}$  and  $R_1$  with MRI-defined cerebellum reference region

Acquisition time	Striatal $BP_{ND}/SUVR-1$		Striatal $R_1$		Cortical $R_1$		Limbic $R_1$	
	$R^2$	Slope	$R^2$	Slope	$R^2$	Slope	$R^2$	Slope
80 min	0.99	1.01	0.94	1.11*	0.64	0.94	0.88	1.11*
40 min	0.95	0.70*	0.94	1.10*	0.71	1.06	0.91	1.13*
30 min	0.91	0.47*	0.93	1.10*	0.68	1.02	0.89	1.17*
20 min	0.85	0.31*	0.89	1.15*	0.59	0.94	0.83	1.28*

\*: Slope significantly different from 1.

similar kinetics of [<sup>11</sup>C]PE2I in these regions as in cerebellum.

Parametric images of  $BP_{ND-SVCA-80}$  and  $R_{1-SVCA-80}$  compared to  $BP_{ND-MRI-80}$  and  $R_{1-MRI-80}$  respectively, are given in **Figure 1B** for one parkinsonian subject and in **Supplemental Figure 1B** for one HC. Visually, the images are very similar, but overall  $R_{1-SVCA-80}$  values were slightly higher than  $R_{1-MRI-80}$  values. The relationships between  $BP_{ND-MRI-80}$  and  $BP_{ND-SVCA-80}$  in striatal regions, and between  $R_{1-MRI-80}$  and  $R_{1-SVCA-80}$  in striatal, cortical and limbic regions are given in **Figure 4A-D** with the corresponding correlations and slope values in **Table 2**. Correlation and agreement between striatal  $BP_{ND-SVCA-80}$  and  $BP_{ND-MRI-80}$  were high ( $R^2=0.99$  and slope =1.01). High correlations were also found between  $R_{1-MRI-80}$  and  $R_{1-SVCA-80}$  in striatal and limbic regions ( $R^2=0.94$  and 0.88 respectively and slope =1.11 for both), whereas only a moderate correlation was noticed for the cortical region ( $R^2=0.64$  and slope =0.94). All correlations were significant ( $P<0.0001$ ).

### Combination of shortened acquisition time and supervised cluster analysis

Parametric images of  $SUVR-1_{SVCA-40}$ ,  $SUVR-1_{SVCA-30}$ ,  $SUVR-1_{SVCA-20}$  and  $R_{1-SVCA-40}$ ,  $R_{1-SVCA-30}$  and  $R_{1-SVCA-20}$  are given in **Figure 1B** for one parkinsonian subject and in **Supplemental Figure 1B** for one HC. The relationships between striatal  $BP_{ND-MRI-80}$  and  $SUVR-1_{SVCA-40}$ ,  $SUVR-1_{SVCA-30}$  and  $SUVR-1_{SVCA-20}$  are given in **Figure 4E**, and between  $R_{1-MRI-80}$  and  $R_{1-SVCA-40}$ ,  $R_{1-SVCA-30}$  and  $R_{1-SVCA-20}$  in striatal, cortical and limbic regions are given in **Figure 4F-H**. Corresponding correlation and slope values are given in **Table 2**.

$SUVR-1_{SVCA-40}$ ,  $SUVR-1_{SVCA-30}$  and  $SUVR-1_{SVCA-20}$  values were underestimated relative to the

$BP_{ND-MRI-80}$  values, but high correlations were found for all scan durations ( $R^2\geq 0.85$ ).  $R_{1-SVCA-40}$ ,  $R_{1-SVCA-30}$ ,  $R_{1-SVCA-20}$  values were slightly overestimated compared to  $R_{1-MRI-80}$  in both striatal and limbic regions but with a high correlation ( $R^2=0.83-0.94$ ) while a lower correlation was found in the cortical region for all scan durations ( $R^2\leq 0.71$ ). Both  $SUVR-1_{SVCA-20}$  and  $R_{1-SVCA-20}$  showed a lower correlation with  $BP_{ND-MRI-80}$  and  $R_{1-MRI-80}$  than the longer scan durations, for all regions.

$BP_{ND}$  and SUVR-1 values in putamen of the two groups separately are shown in **Figure 5A** for the full 80 min data with both MRI- and SVCA-based reference region, and for the shortened data sets with SVCA-based reference. There was a significant difference between the groups for all scan durations ( $p<0.0001$ ). The effect size (Cohen's d) is shown in **Figure 5B**. Cohen's d values were  $\geq 4$  for all acquisition times with SVCA-based reference, indicating a high degree of discrimination between patients with parkinsonism and HC in the complete and shortened datasets.

### Discussion

In this study, a clinically feasible scan protocol and analysis method for dynamic [<sup>11</sup>C]PE2I PET data were evaluated. Previous studies have shown that parametric images of dynamic [<sup>11</sup>C]PE2I data can be computed using RPM [10], a basis function implementation of SRTM. It has also been shown that parametric  $BP_{ND}$  and  $R_1$  images of a single PET scan with [<sup>11</sup>C]PE2I can be used in the differential diagnosis for patients with parkinsonism, giving essentially the same information as a dual scan approach to assess DAT availability and overall brain functional activity in two separate scans with [<sup>123</sup>I]FP-CIT SPECT and [<sup>18</sup>F]FDG PET [11]. Major drawbacks for clinical use of [<sup>11</sup>C]PE2I, especially for patients suffering from neurodegenerative diseases and movement disorders, are the long scan time required and the need for a structural MRI for reference region definition, which involve an additional scan for the patient and additional cost for the health care system. To address these



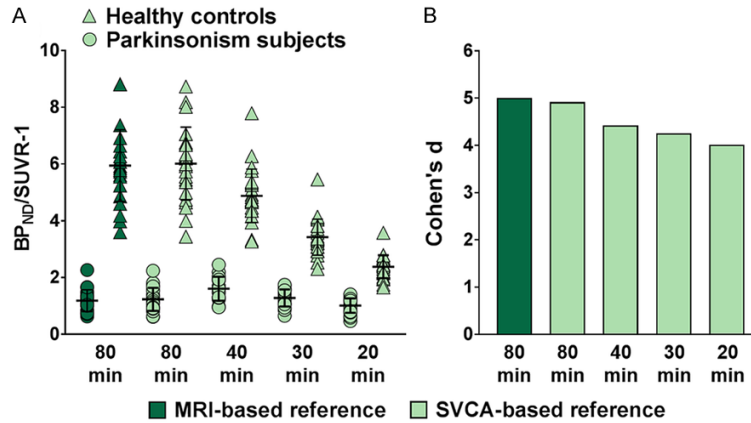


**Figure 5.** A.  $\text{BP}_{\text{ND}}$  values of the full 80 min acquisition time, with both MRI- and SVCA-based reference region, and SUVR-1 values of 40, 30 and 20 min scan duration in putamen, with SVCA-based reference region, for the healthy controls and the subjects with parkinsonism. Horizontal bars showing mean and standard deviation of the mean. B. Standardized difference of the mean (Cohen's  $d$ ) of  $\text{BP}_{\text{ND}}$  and SUVR-1 values in putamen between subjects with parkinsonism and healthy controls for varying scan durations.

issues, validation of a shorter scan acquisition time for [ $^{11}\text{C}$ ]PE2I and a supervised clustering method to obtain a reference TAC directly from the dynamic PET data was reported in this paper.

As mentioned in the introduction, SUVR correspond best to  $\text{BP}_{\text{ND}}$  during transient equilibrium which is the time at which the specific binding, calculated as the difference between putamen and cerebellum curves, peaks. For [ $^{11}\text{C}$ ]PE2I, this difference is approximately constant after 30 min p.i., which supports the use of the 30-40 min interval for measurement of SUVR. However, transient equilibrium is reached faster in patients than in subjects without neurodegeneration in putamen, which explains the relatively larger underestimation of SUVR-1 relative to  $\text{BP}_{\text{ND}}$  in the control group compared to the patient group, and hence the reduced discrimination between groups for shorter scan durations as shown in **Figure 5A**.

Shorter scan durations led to decreasing correlation and agreement between SUVR-1 values and  $\text{BP}_{\text{ND}}$  values based on an 80 min acquisition time, irrespective of the use of an MRI-based or SVCA-based reference region. The relative importance of this should be seen in terms of how well each method can discriminate between subjects with normal and abnormal DAT function. As **Figure 5B** shows, Cohen's

$d$  is equal to or larger than 4 for all scan durations, indicating that there is a probability of less than 5% that SUVR-1 of a patient with an appreciable degeneration of DAT availability in putamen falls within the 95% confidence interval of the control group. This result should, however, be considered with some caution as the mean age of the patients with parkinsonism was significantly higher than the control group. Previous PET studies have reported an age-related decline of striatal DAT of about 6-8% per decade [20, 21] which would have decreased the difference between the two groups if they had been of the same

age. Even though we could have corrected our  $\text{BP}_{\text{ND}}$  values for the age difference we do not know the exact effect of age on SUVR. However, a scan duration of 40 min still appeared to be sufficient for discrimination between groups with and without neurodegeneration in putamen but further studies are needed with age-matched controls. Previous studies have also reported a gender difference in DAT availability in both PD [22] and controls [23], with female subjects exhibiting greater DAT activities in striatal region but also a possible greater age-related decline than men. This is not considered in the present work due to the limited sample size and we do not believe such effects would affect our conclusions.

Scan durations as short as 20 min did not affect the quantitative accuracy of  $R_1$  values to any major extent as long as an MRI-based reference region was used (**Figure 2**). Cortical  $R_1$  values based on an SVCA reference region, however, correlated only moderately with those estimated using an MRI-based reference region, especially for 20 min scan duration. One reason for the lower correlation in cortical  $R_1$  values compared to striatal and limbic values is the relatively narrow range of cortical  $R_1$  values and the fact that the SVCA-based reference region includes a large number of cortical voxels (**Figure 3B**) may also be of importance. However, the correlation between MRI- and

SVCA-based cortical  $R_1$  values within-subject as opposed to the across-subject correlations shown in **Table 2**, was 0.99 on average (range 0.96-1.00) for scan durations down to 30 min and slightly lower, 0.98, for 20 min. As we have previously shown,  $R_1$  images based on 80 min [<sup>11</sup>C]PE2I data correlated strongly with [<sup>18</sup>F]FDG images [11].  $R_1$  images based on shorter scan duration of [<sup>11</sup>C]PE2I and with SVCA-based reference need to be further evaluated in clinical data and compared to [<sup>18</sup>F]FDG images. The high within-subject correlation between SVCA- and MRI-based  $R_1$  values in cortex, independent of scan duration, suggests that the ability to discriminate between different parkinsonian syndromes is unaffected by shorter scan durations and the use of SVCA.

The SVCA reference region extraction has previously been proposed for a number of different brain PET tracers [13-17]. The method has proven useful in tracers where a specific reference tissue is difficult to define, as for example in [<sup>11</sup>C]PK11195, as well as for tracers where a reference region does exist, for example in [<sup>11</sup>C]PIB and as shown here for [<sup>11</sup>C]PE2I. A possible challenge of SVCA is that the timing and speed of the bolus injection, as well as the characteristics of the PET scanner and reconstruction method, may affect the relative shapes of the TACs making similar tracer administration, data acquisition, and data pre-processing routines important.

One parkinsonian patient showed a significant cerebellar neurodegeneration and was identified as having MSA with atrophy related to cerebellum [11]. As a consequence of using an MRI-defined cerebellum VOI as reference region, the  $R_1$  values were significantly above average. When using an SVCA-based reference TAC, the  $R_1$  values were no longer overestimated. This indicates that the part of cerebellum suffering from neurodegeneration was not included in the SVCA-based reference region due to a different kinetics and that an advantage of SVCA is that it can be used to overcome such biases in the  $R_1$  estimates.

Another possibility for acquiring both DAT availability and overall brain functional activity based on a single administration of [<sup>11</sup>C]PE2I would be a scan approach where the patient is scanned for 20 min p.i. to measure  $R_1$ , followed by a second scan between 60 and 80 min p.i.

to measure SUVR. As we have demonstrated previously, agreement between 80 min  $BP_{ND}$  and SUVR-1 at 60-80 min p.i. with MRI-based reference is slightly better than at the earlier intervals assessed in the present work [10]. However, this would both complicate patient logistics and automated analysis because of the need for additional co-registration between the early and late scans. In addition, an equal correlation is found between  $BP_{ND-MRI-80}$  and  $SUVR-1_{SVCA-40}$  and the separation between the parkinsonism group and the control group appears sufficient at this time interval.

A challenge associated with the clinical implementation of [<sup>11</sup>C]PE2I is that it can only be used at a PET-facility with on-site production because of the 20.4 min <sup>11</sup>C half-life, in contrast to [<sup>123</sup>I]FP-CIT or <sup>18</sup>F-labelled DAT ligands such as [<sup>18</sup>F]FE-PE2I [24]. On the other hand, differential diagnosis of parkinsonism generally takes place at specialized hospitals, which often have access to a cyclotron. In addition, the use of a [<sup>11</sup>C]PE2I scan results in about 70% reduction of radiation exposure to the patients compared to the dual scan approach with [<sup>18</sup>F]FDG and [<sup>123</sup>I]FP-CIT [11], but also compared to a scan with [<sup>18</sup>F]FE-PE2I using the same amount of radioactivity [25].

## Conclusion

An acquisition time of 40 min is sufficient for generating quantitatively accurate parametric [<sup>11</sup>C]PE2I SUVR-1 and  $R_1$  images, showing DAT availability and overall brain functional activity with high correlation to those based on 80 min acquisition time. Furthermore, SVCA provided an automated method for extracting a reliable reference TAC directly from the dynamic [<sup>11</sup>C]PE2I with a high agreement compared to an MRI-based reference for both SUVR-1 and  $R_1$ . SUVR-1 values based on 40 min [<sup>11</sup>C]PE2I data and with SVCA extracted reference TAC could adequately discriminate between control subjects and parkinsonian patients suffering from degeneration of DAT availability in putamen.

## Acknowledgements

The authors would like to thank the staff at the PET centre at Uppsala University Hospital for the production of [<sup>11</sup>C]PE2I and for the acquisition of the PET data. This work was in part

financed by grants from Uppsala University Hospital, the regional agreement on medical training and clinical research (ALF) between Uppsala County Council and Uppsala University, the Swedish Parkinson Foundation (Jens Sörensen) and the Swedish Research Council (Tomas Furmark). Andreas Frick is supported by the Swedish Society for Medical Research (SSMF).

#### Disclosure of conflict of interest

None.

**Address correspondence to:** My Jonasson, Medical Physics, Uppsala University Hospital, 751 85 Uppsala, Sweden. E-mail: my.jonasson@radiol.uu.se

#### References

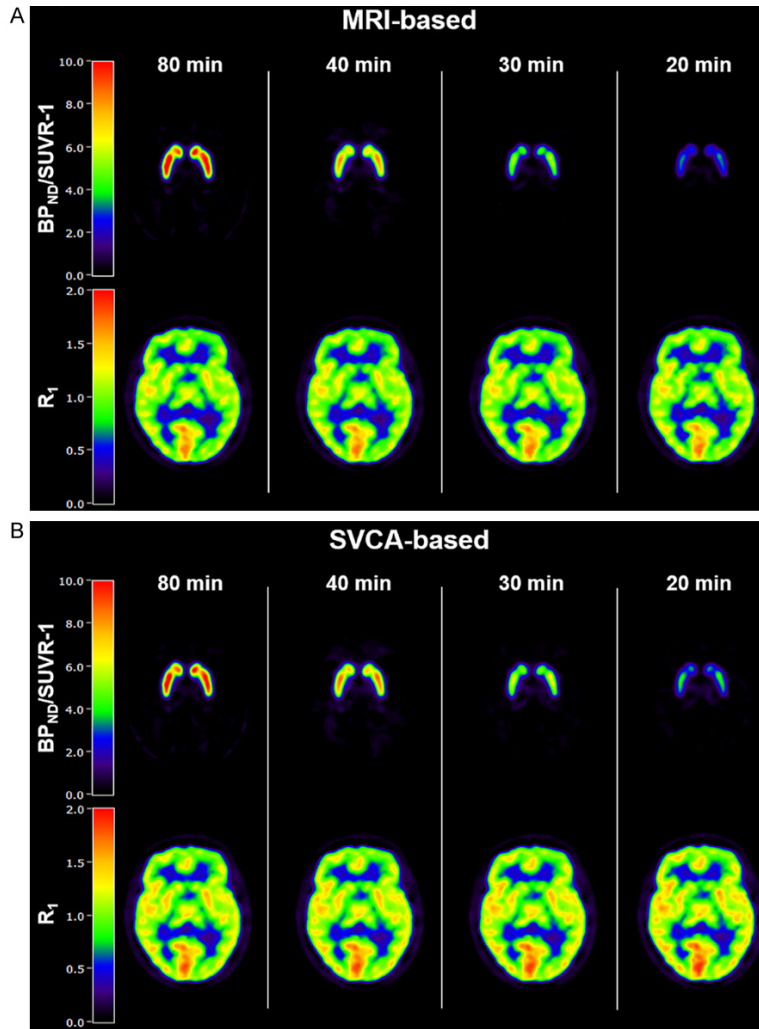
- [1] Antonini A, Moresco RM, Gobbo C, De Notaris R, Panzacchi A, Barone P, Calzetti S, Negrotti A, Pezzoli G and Fazio F. The status of dopamine nerve terminals in Parkinson's disease and essential tremor: a PET study with the tracer [<sup>11</sup>C]FE-CIT. *Neurol Sci* 2001; 22: 47-48.
- [2] Ribeiro MJ, Vidailhet M, Loc'h C, Dupel C, Nguyen JP, Ponchant M, Dollé F, Peschanski M, Hantraye P, Cesaro P, Samson Y and Remy P. Dopaminergic function and dopamine transporter binding assessed with positron emission tomography in Parkinson disease. *Arch Neurol* 2002; 59: 580-586.
- [3] DeLorenzo C, Kumar JS, Zanderigo F, Mann JJ and Parsey RV. Modeling considerations for in vivo quantification of the dopamine transporter using [<sup>11</sup>C]PE2I and positron emission tomography. *J Cereb Blood Flow Metab* 2009; 29: 1332-1345.
- [4] Hirvonen J, Johansson J, Teräs M, Oikonen V, Lumme V, Virsu P, Roivainen A, Någren K, Halldin C, Farde L and Hietala J. Measurement of striatal and extrastriatal dopamine transporter binding with high-resolution PET and [<sup>11</sup>C]PE2I: quantitative modeling and test-retest reproducibility. *J Cereb Blood Flow Metab* 2008; 28: 1059-1069.
- [5] Jucaite A, Odano I, Olsson H, Pauli S, Halldin C and Farde L. Quantitative analyses of regional [<sup>11</sup>C]PE2I binding to the dopamine transporter in the human brain: a PET study. *Eur J Nucl Med Mol Imaging* 2006; 33: 657-668.
- [6] Seki C, Ito H, Ichimiya T, Arakawa R, Ikoma Y, Shidahara M, Maeda J, Takano A, Takahashi H, Kimura Y, Suzuki K, Kanno I and Suhara T. Quantitative analysis of dopamine transporters in human brain using [<sup>11</sup>C]PE2I and positron emission tomography: evaluation of reference tissue models. *Ann Nucl Med* 2010; 24: 249-260.
- [7] Zheng M, Appel L, Luo F, Lane R, Burt D, Risinger R, Antoni G, Cahir M, Keswani S, Hayes W and Bhagwagar Z. Safety, pharmacokinetic, and positron emission tomography evaluation of serotonin and dopamine transporter occupancy following multiple-dose administration of the triple monoamine reuptake inhibitor BMS-820836. *Psychopharmacology (Berl)* 2015; 232: 529-540.
- [8] Lammertsma AA and Hume SP. Simplified reference tissue model for PET receptor studies. *Neuroimage* 1996; 4: 153-158.
- [9] Gunn RN, Lammertsma AA, Hume SP and Cunningham VJ. Parametric imaging of ligand-receptor binding in PET using a simplified reference region model. *Neuroimage* 1997; 6: 279-287.
- [10] Jonasson M, Appel L, Engman J, Frick A, Nyholm D, Askmark H, Danfors T, Sörensen J, Furmark T and Lubberink M. Validation of parametric methods for [<sup>11</sup>C]PE2I positron emission tomography. *Neuroimage* 2013; 74: 172-178.
- [11] Appel L, Jonasson M, Danfors T, Nyholm D, Askmark H, Lubberink M and Sörensen J. Use of <sup>11</sup>C-PE2I PET in differential diagnosis of parkinsonian disorders. *J Nucl Med* 2015; 56: 234-242.
- [12] Ito H, Hietala J, Blomqvist G, Halldin C and Farde L. Comparison of the transient equilibrium and continuous infusion method for quantitative PET analysis of [<sup>11</sup>C]raclopride binding. *J Cereb Blood Flow Metab* 1998; 18: 941-950.
- [13] Turkheimer FE, Edison P, Pavese N, Roncaroli F, Anderson AN, Hammers A, Gerhard A, Hinz R, Tai YF and Brooks DJ. Reference and target region modeling of [<sup>11</sup>C]-(R)-PK11195 brain studies. *J Nucl Med* 2007; 48: 158-167.
- [14] Yaqub M, van Berckel BN, Schuitemaker A, Hinz R, Turkheimer FE, Tomasi G, Lammertsma AA and Boellaard R. Optimization of supervised cluster analysis for extracting reference tissue input curves in (R)-[<sup>11</sup>C]PK11195 brain PET studies. *J Cereb Blood Flow Metab* 2012; 32: 1600-1608.
- [15] Ikoma Y, Edison P, Ramlackhansingh A, Brooks DJ and Turkheimer FE. Reference region automatic extraction in dynamic [<sup>11</sup>C]PIB. *J Cereb Blood Flow Metab* 2013; 33: 1725-1731.
- [16] Lyoo CH, Zanotti-Fregonara P, Zoghbi SS, Liow JS, Xu R, Pike VW, Zarate CA, Fujita M and Innis RB. Image-derived input function derived from a supervised clustering algorithm: methodology and validation in a clinical protocol using [<sup>11</sup>C](R)-rolipram. *PLoS One* 2014; 9: e89101.
- [17] Rissanen E, Tuisku J, Luoto P, Arponen E, Johansson J, Oikonen V, Parkkola R, Airas L and Rinne JO. Automated reference region extraction and population-based input function for brain [<sup>11</sup>C]TMSX PET image analyses. *J Cereb Blood Flow Metab* 2015; 35: 157-165.

## Clinically feasible [<sup>11</sup>C]PE2I PET

- [18] Halldin C, Erixon-Lindroth N, Pauli S, Chou YH, Okubo Y, Karlsson P, Lundkvist C, Olsson H, Guilloteau D, Emond P and Farde L. [<sup>11</sup>C]PE2I: a highly selective radioligand for PET examination of the dopamine transporter in monkey and human brain. *Eur J Nucl Med Mol Imaging* 2003; 30: 1220-1230.
- [19] Svarer C, Madsen K, Hasselbalch SG, Pinborg LH, Haugbøl S, Frøkjær VG, Holm S, Paulson OB and Knudsen GM. MR-based automatic delineation of volumes of interest in human brain PET images using probability maps. *Neuroimage* 2005; 24: 969-979.
- [20] Volkow ND, Ding YS, Fowler JS, Wang GJ, Logan J, Gatley SJ, Hitzemann R, Smith G, Fields SD and Gur R. Dopamine transporters decrease with age. *J Nucl Med* 1996; 37: 554-559.
- [21] Shingai Y, Tateno A, Arakawa R, Sakayori T, Kim W, Suzuki H and Okubo Y. Age-related decline in dopamine transporter in human brain using PET with a new radioligand [<sup>18</sup>F]FE-PE2I. *Ann Nucl Med* 2014; 28: 220-226.
- [22] Lee JJ, Ham JH, Lee PH and Sohn YH. Gender differences in age-related striatal dopamine depletion in Parkinson's disease. *J Mov Disord* 2015; 8: 130-135.
- [23] Varrone A, Dickson JC, Tossici-Bolt L, Sera T, Asenbaum S, Booij J, Kapucu OL, Kluge A, Knudsen GM, Koulibaly PM, Nobili F, Pagani M, Sabri O, Vander Borght T, Van Laere K and Tatsch K. European multicentre database of healthy controls for [<sup>123</sup>I]FP-CIT SPECT (ENC-DAT): age-related effects, gender differences and evaluation of different methods of analysis. *Eur J Nucl Med Mol Imaging* 2013; 40: 213-227.
- [24] Varrone A, Steiger C, Schou M, Takano A, Finnema SJ, Guilloteau D, Gulyás B and Halldin C. In vitro autoradiography and in vivo evaluation in cynomolgus monkey of [<sup>18</sup>F]FE-PE2I, a new dopamine transporter PET radioligand. *Synapse* 2009; 63: 871-880.
- [25] Varrone A, Gulyás B, Takano A, Stabin MG, Jonsson C and Halldin C. Simplified quantification and whole-body distribution of [<sup>18</sup>F]FE-PE2I in nonhuman primates: prediction for human studies. *Nucl Med Biol* 2012; 39: 295-303.



# Clinically feasible [<sup>11</sup>C]PE2I PET



**Supplemental Figure 1.** Parametric [<sup>11</sup>C]PE2I images of a healthy control. A. Comparison of BP<sub>ND</sub> and SUVR-1 images (top row) and R<sub>1</sub> images (bottom row) of different scan durations with an MRI-based reference region. B. BP<sub>ND</sub> and SUVR-1 images (top row) and R<sub>1</sub> images (bottom row) of different scan duration with an SVCA-based reference region.

**Supplemental Table 1.** Residual sum of squares (RSS), square of Pearson's correlation coefficient (R<sup>2</sup>), slope of orthogonal regression and bias of BP<sub>ND</sub> and R<sub>1</sub> with SVCA-based reference region with different thresholds relative to 80 min BP<sub>ND</sub> and R<sub>1</sub> with MRI-defined cerebellum reference region

SVCA-based threshold	Striatal BP <sub>ND</sub>				Striatal, cortical and limbic R <sub>1</sub>		
	RSS	R <sup>2</sup>	Slope	Bias ± SD	R <sup>2</sup>	Slope	Bias ± SD
0.7	62.92	0.99	1.01	-0.03 ± 0.25	0.89	1.13*	-0.10 ± 0.06
0.8	45.28	0.99	1.01	-0.06 ± 0.27	0.88	1.09*	-0.08 ± 0.06
0.9	31.24	0.98	1.02	-0.10 ± 0.29	0.88	1.06*	-0.05 ± 0.06
0.95	27.25	0.98	1.02	-0.15 ± 0.30	0.87	1.04*	-0.04 ± 0.06
1	27.08	0.98	1.03	-0.23 ± 0.31	0.85	1.03	-0.03 ± 0.06

\*: slope significantly different from 1.